Multiscale organisation of lead carboxylates in artistic oil binders

Lucie Laporte, Frederic Gobeaux, Thierry Pouget, Nicolas Benoot, Julien Foisnon, David Touboul, Guylaine Ducouret, Laurence de Viguerie

Multiscale organisation of lead carboxylates in artistic oil binders

Lucie Laporte [a], Frédéric Gobeaux [b] , Thierry Pouget [c], Nicolas Benoot [c], Julien Foisnon [d], David Touboul [e,] Guylaine Ducouret [f], Laurence de Viguerie [a]*

[a] Laboratoire d'Archéologie Moléculaire et Structurale (LAMS), CNRS UMR 8220, Sorbonne Université, 75005, Paris, France
[b] Université Paris-Saclay, CNRS, CEA, NIMBE, LIONS, 91191 Gif-sur-Yvette, France
[c] LVMH Research, Helios Research Center, Materials Innovation Department, 45800 Saint-Jean-de-Braye, France
[d] Laboratoire de Chimie Moléculaire (LCM), CNRS, École polytechnique, Institut Polytechnique de Paris, 91120 Palaiseau, France
[e] Université Paris-Saclay, CNRS, Institut de Chimie des Substances Naturelles, UPR 2301, 91198 Gif-sur-Yvette, France
[f] Laboratoire Science et Ingénierie de la Matière Molle (SIMM), CNRS UMR 7615, ESPCI Paris, PSL Research University, Sorbonne Université, 75005, Paris, France

*Corresponding author: laurence.de_viguerie@sorbonne-universite.fr

Graphical abstract

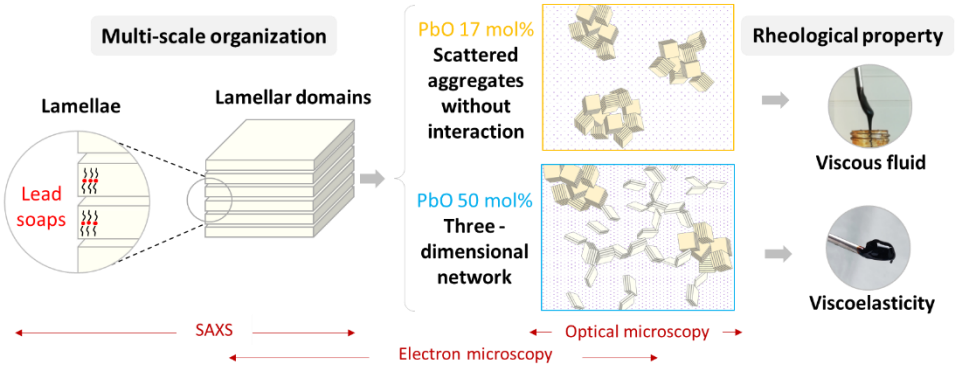

Abstract

The supramolecular and mesoscopic architectures of lead-saponified linseed oil, used by painters since the Renaissance, have been characterised and linked to their rheological properties. The multi-scale organization of saponified oils has been demonstrated by SAXS (Small angle X-ray Scattering), FF-TEM (Freeze-Fracture Transmission Electron Microscopy) and DIC (Differential Interference Contrast): some of the lead soaps (formed when the oil is heated in the presence of PbO) are organized into microscopic lamellar domains, distributed in a continuous matrix made up of unorganized species (partially saponified triglycerides, glycerol, remaining soaps, etc.). The concentration of lead soaps in the oil controls the average size and interaction between the lamellar domains. Linseed oil + PbO 17 mol% is viscous and consists of aggregates of lamellar domains isolated within the continuous unorganized matrix. In contrast, in linseed oil + PbO 50 mol%, the domains are homogeneously dispersed and form what can be described as a three-dimensional network, giving the system viscoelastic properties.

Keywords

Lead soaps, Small angle X-ray Scattering (SAXS), microscopy, self-assembled systems, viscoelasticity

Introduction

From the Renaissance onwards, the technique of oil painting spread throughout Europe, based on the grinding of pigments with natural drying oils, such as linseed, walnut or poppy seed oils. To speed up their drying process, the use of metallic driers seems to have given good results and became common practice among painters, a practice that continues to this day. A common treatment was to heat the oil with metal oxides, the most commonly used being lead (II) oxide PbO [1]. This treatment leads to the partial saponification of the triglycerides of the oil and to the formation of metal soaps, which consist of two long-chain carboxylate anions $R\text{-}COO^-$ (R being a linear saturated or unsaturated carbon chain) complexed with a divalent metal cation of lead Pb^{2+} [2]. Metal soaps are formed from the aliphatic chains of triglycerides, the most common of which are shown below (Table 1).

The presence of metallic soaps significantly modifies the oils' properties, not only their drying capacity but also their rheological properties (viscosity, viscoelasticity) [3–5]. The painters could therefore adjust the consistency and workability of their oils to suit their needs [6,7]. The kinetics of oxidation and cross-linking of the triglycerides, which are necessary steps for the formation of a solid and durable film, are accelerated by the presence of metallic driers [3,8–11]. However the presence of lead soaps is also associated to long-term conservation issues, such as the formation of the so-called protrusions which are micrometric aggregates of saturated organized lead soaps identified in artworks that are centuries old, creating irreversible damages [12–17].

Clarifying the structuring of saponified oils is a key step in understanding how lead soaps modify the properties of paints before and during drying (i.e. polymerization of the film-forming compounds). Several works on pure systems have shown that saturated soaps based on lead, zinc, copper, cobalt and silver have the ability to self-assemble into lamellae [18–22]. Monounsaturated soaps, such as lead and zinc oleates (C18:1) also form lamellar structures with reduced thickness compared to the equivalent saturated soaps, due to the kink formed by the double bond [23,24]. Cohesion is favored for saturated aliphatic chains, for which van der Waals interactions are maximized. In the case of vegetable oils used as a binder for paints, such as linseed and walnut oils, the main components are triglycerides of C16 and C18 fatty acids chains, saturated, and mostly polyunsaturated [25,26]. Heating the oil with lead oxide induce the partial saponification of these triglycerides, i.e. the formation of saturated, mono- and mainly polyunsaturated lead carboxylates. A significant fraction of un-saponified molecules (tri-, di- and monoglyceride) remains in the system, as well as products of additional reactions induced by the heating process, such as oxidation [27], isomerization [28,29], cleavage [30] and oligomerization [31]. All these molecules form a complex "oil matrix". Considering the diversity of the fatty chains and the "oil matrix" seems essential to describe the structuring of saponified oils.

Table 1 : Names and formulas of the main aliphatic chains of vegetable oil triglycerides used in paint. An example of a triglyceride (1-palmitoyl-2-linoleoyl-3-oleoyl-glycerol) is represented on the right. The green part on the triglyceride corresponds to the glycerol residue.

Fatty acids chains		Triglyceride
Name	**Formula**	
Palmitic (C16:0)		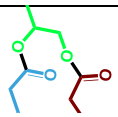

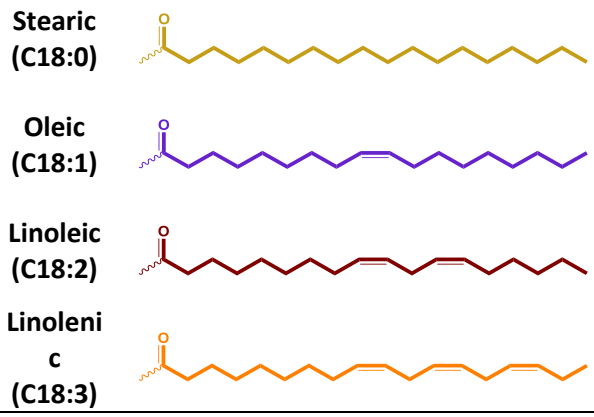

The aim of this study was to identify the supramolecular and mesoscopic organization of the saponified oils formulated according to historical recipes (based on linseed oil and lead (II) oxide PbO [32]). We used SAXS (Small Angle X-ray Scattering) measurements and microscopy to describe their architecture, focusing on the results obtained for two model formulations of linseed oil + PbO 17 and 50 mol%. SAXS analyses provided access to the supramolecular organization of the systems. FF-TEM (Freeze-Fracture Transmission Electron Microscopy) enabled the visualization of the internal structure of the saponified oils at the micron scale (0.1 µm - 10 µm). In addition, DIC (Differential Interference Contrast) microscopy gave information on the structuring at a scale ranging from 1 to 100 µm. Complementary measurements of viscoelasticity and chemical composition are provided to interpret the obtained results.

Material and Methods

Formulation of saponified oils

The used linseed oil was untreated cold pressed oil from Kremer (ref. 73020). The composition of fatty acids is given by the provider as: linolenic acid 61.3 %, oleic acid 15.3 %, linoleic acid 14.6 %, palmitic acid 4.4 %, stearic acid 2.9 % plus others minor compounds (arachidic acid 0.1 %, gadoleic acid 0.1 %, lignoceric acid 0.2%, nervonic acid 0.3 %). To investigate the influence of the initial PbO concentration, formulations containing 1, 5, 10, 20 and 25 wt% PbO (corresponding respectively to 4, 17, 31 and 50 and 57 mol% PbO) were prepared. The samples were formulated in batches of 20 g. Lead (II) oxide PbO (Emsure) was first pre-ground with 2 mL of linseed oil in a porcelain mortar for 20 s. The remaining oil was then added and the mixture was ground for 40 additional seconds. The mixture was transferred to a 100 mL beaker and heated in a silicone oil bath at a control temperature of 150°C, with magnetic stirring. At the end of heating, the treated oil was immediately poured into a glass pillbox, left to cool at ambient temperature, and the saponification rate τ_S (i.e. the percentage of saponified ester bonds) was determined by FTIR (Fourier Transform InfraRed spectroscopy), following a method described in detail elsewhere [2], with 3 measurements per sample. All saponification rates are given in Supporting Information, Table S1. GC-MS (Gas Chromatography – Mass Spectrometry) measurements were also performed on linseed oil + PbO 17 and 50 mol% to quantify and compare the lead soaps and free fatty acids formed during processing (see Supporting Information Figure S1). To avoid any effect related to the aging of samples, the analyses presented below were performed on ‘‘fresh” samples, apparently homogeneous, at the latest ten days after formulation. Between measurements, the samples were stored at 4°C in sealed pillboxes under inert gas (N_2).

Rheology

Oscillatory measurements were performed to assess the viscoelasticity of the saponified oils. Measurements were carried out on a HAAKE MARS 40 controlled stress rheometer (Thermo Fisher Scientific), equipped with a sand blasted stainless steel cone-plate geometry (diameter: 35 mm, angle: 2°; gap: 0.104 mm). A strain sweep test from 0.05 to 1000 % strain was carried out at f = 1 Hz to evaluate the extent of the linear regime. When samples were viscoelastic, a frequency sweep test from 0.1 to 20 rad/s was performed in the linear viscoelastic plateau at constant strain of 0.1 % on a new sample, in order to describe the time-dependent behavior of the saponified oil in the non-destructive deformation range identified by the strain sweep. Measurements were done at 25 °C, the temperature being maintained by an air Peltier module. Each measurement was repeated at least twice to check reproducibility. A duplicate sample with the same composition, prepared in the same conditions, was also analyzed and its properties compared to the first one.

SAXS (Small angle X-ray Scattering)

Preparation of samples

The oils were transferred into cylindrical quartz capillaries of 1 mm outer diameter and 0.01 mm thickness (Hilgenberg). The samples were introduced into the capillaries using a syringe and a 0.8 mm diameter needle. When samples were too viscous to be introduced by syringe (e.g. 50 mol% PbO), a centrifuge Sigma 2-16P was used at 2000 rpm for 1 min. Acquisitions were done at several positions in the capillary to ensure that centrifugation did not result in heterogeneous structuring of the sample. Capillaries were then sealed with a blowtorch.

Experimental Conditions

The measurements were performed at room temperature at the SOLEIL synchrotron on the SWING beamline: the samples were irradiated by a 12 keV beam. The scattered intensity was collected by an EigerX4M detector (Dectris) with a 75x75 mm^2 pixel size (10 frames acquisition per image, 1000 ms of exposure time). For each sample, 10 images were recorded and averaged. Two sample-detector distances of 0.5 m and 6 m were used. In such condition, the accessible q range, q being the scattering vector ($q = 4\pi sin\theta/\lambda$) where 2θ is the scattering angle and λ the wavelength) extends from 0.002 to 0.6 $Å^{-1}$ after mask application. The obtained images were treated with Foxtrot 3.5 using an angular integration from 0 to 360°. Such a procedure yields curves in which the scattered intensity is plotted versus the scattering vector modulus q. Because of the uncertainty in the capillary diameter, we considered the scattered intensity in arbitrary units (a.u.).

Microscopy

FF-TEM (Freeze-Fracture Transmission Electron Microscopy)

The samples were prepared using a BAF060 device from LEICA: they were frozen directly in liquid propane cooled to liquid nitrogen temperature, and knife-fractured at -125°C, under vacuum ($1.6x10^{-6}$ mbar). The cut surface was then coated with a layer of 4 nm platinum and 40 nm carbon. The resulting replicas were washed with a 50/50 mixture of tetrahydrofuran (THF) and chloroform to remove the sample underneath and then transferred on copper TEM grids (AGS160-4 carbon-coated grids Cu 400, from Oxford Instruments). Visualizations were performed at room temperature on a CM 120 - FEI TEM (Thermo Fisher Scientific) equipped with a LaB6 (lanthanum hexaboride) source, at an acceleration voltage of 120 kV. The images were collected using a CCD camera (resolution 1300x1030), from GATAN, with an exposure time of between 0.3 seconds and 2 seconds. The images were acquired and processed using Digital Micrograph software suite from GATAN.

DIC (Differential Interference Contrast) microscopy

DIC microscopy is used to enhance the contrast of transparent samples, such as oils. Adjacent areas with different refractive indices appear contrasted, giving the appearance of a three-dimensional physical relief. Observations were performed in transmission between slide and coverslip on an Axio Imager 2 microscope (Zeiss) with a white light source.

Results

Viscoelasticity

Rheology of saponified oils have previously been investigated and presented in detail in [5]. The main results obtained for linseed oils + PbO 17 and 50 mol% (leading respectively to saponification rates τ_S of 18 ± 2 % and 59 ± 4 %) are summarized below and the behavior of oils with higher saponification rate (57 mol%, τ_S = 72 ± 1) is described. Linseed oil + PbO 50 mol% exhibited viscoelastic properties whereas viscous behavior predominated in the linseed oil + PbO 17 mol% sample, as *G'* was lower than *G''* over the entire strain range tested (see Supporting Information Figure S2.a). Linseed oil + PbO 50 mol% exhibited a linear viscoelastic plateau located between 0.05 and 0.5 % strain (Figure 1.a). From 0.5% strain, *G'* and *G''* started to decrease and then crossed each other at around 2 % strain. Additional frequency sweep test on the viscoelastic plateau (Figure 1.b, strain $\gamma = 0.1\%$) revealed that *G'* was higher than *G''* over the whole frequency range studied, and the two moduli increased as a function of the frequency according to a power law of exponent 0.27 (*G'*) and 0.34 (*G''*). Surprisingly, when the PbO content was higher than 50 mol%, the viscoelastic properties were not enhanced as one would have expected but linseed oil + PbO 57 mol% was not viscoelastic (see Supporting Information, Figure S2.b)

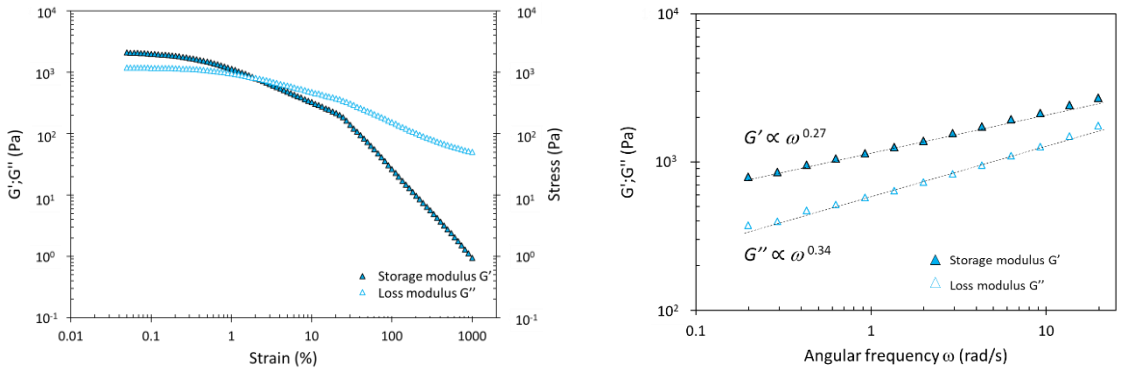

(a) (b)

Figure 1 : (a) Oscillatory strain sweep test on linseed oil + PbO 50 mol% from 0.05 to 1000 % (f = 1 Hz). (b) Oscillatory frequency sweep on linseed oil + PbO 50 mol%, from 20 to 0.1 rad/s (strain = 0.1%).

To clarify the origin of these distinct rheological behaviors, a closer look on the organization of saponified oils was necessary.

Organization

SAXS (Small angle X-ray Scattering)

The Figure 2.a displays the scattered intensity profiles as a function of the scattering vector *q* for linseed oil samples heated with 0 up to 57 mol% PbO.

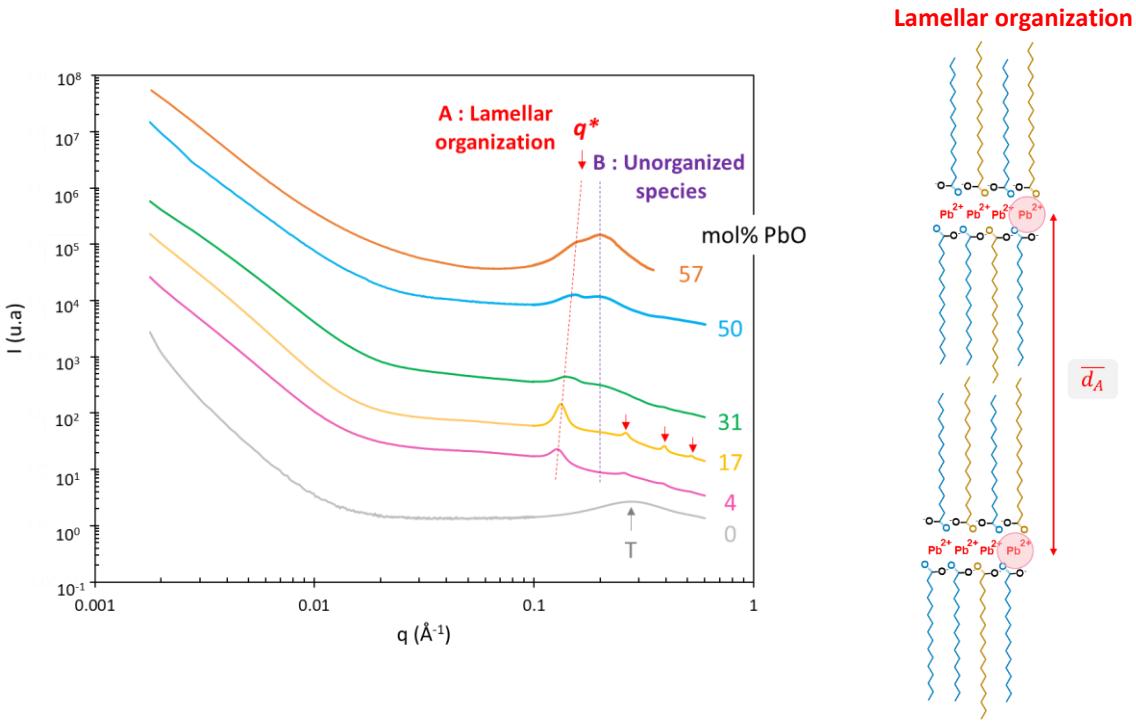

Figure 2 : (a) Scattered intensity profiles as a function of the scattering vector q for oils heated with 0 to 57 mol% PbO from 0.002 to 0.6 Å^{-1}. Data were normalized in transmission and the empty capillary signal was subtracted. The broad peak observed on the linseed oil profile, corresponding to the correlation distance between polar cores of the triglycerides, is noted T. The two contributions observed on the profiles of the saponified oils are noted A and B. Red arrows indicate periodic oscillations characteristic of local lamellar organization, with q the position of the first oscillation. For the linseed oil + PbO 57 mol%, the data are displayed from 0.01 to 0.35 Å^{-1}, due to a mask defect. (b) Scheme of the lamellar organization. The lead soaps shown are saturated, with C16:0 (palmitic, in blue) and/or C18:0 (stearic, in light brown) chains.*

Table 2 : Evolution of the characteristic distances $\bar{d}$ of the contributions A and B and the correlation length of the lamellar domains ξ as a function of the initial PbO concentration.

mol% PbO	4	17	31	50	57
$\overline{d_A}$ (Å)	49	47	44	42	40
$\overline{d_B}$ (Å)	30	30	31	30	30
ξ (Å)	267	382	176	171	174

Linseed oil did not show any particular organization: only a broad peak, centered at q = 0.28 Å^{-1}, was visible. This signal has been previously observed on other types of vegetable oils. The position of this peak corresponds to the average correlation distance between the glycerol residues of the triglycerides ($\overline{d_T} = 2\pi/q_{max} = 23$ Å) [33].

The signals of the saponified oils significantly differed from that of the reference linseed oil. Dominated by the elastic scattering of lead atoms, they provide information on the structuring of the lead soaps contained in the formulations. The profile of linseed oil + 17 mol% PbO showed a series of periodically spaced oscillations with a position ratio of 1:2:3:4. These oscillations can be assigned to a lamellar organization (noted A, in red, represented schematically in Figure 2.b), whose characteristic

distance is given by $\overline{d_A} = 2\pi/q^*$, *i.e.* 47 Å for linseed oil + PbO 17 mol% (with *q** the position of the first oscillation, located at 0.13 $Å^{-1}$).

Moreover, a broad signal, centered at 0.20 $Å^{-1}$ (noted B, in black) was also visible. This liquid order signal may originate from unorganized species in particular lead soaps, with a correlation distance between lead centers of $\overline{d_B} = 30$ Å.

Variations of these two signals were observed depending on the lead content. The broad liquid order signal B increased with the initial proportion of PbO: it was not pronounced for linseed oil + PbO 17 mol% but dominated the profile for linseed oil + PbO 50 mol%. The proportion of unorganized species is thus more important in the highly saponified samples.

The periodically spaced oscillations, width and position, also depended on the initial PbO concentration. The characteristic distance $\overline{d_A}$ decreased with increasing initial PbO content (hence saponification rate): it was 44, 42 and 40 Å respectively for linseed oil + PbO 31, 50 and 57 mol% (Table 2).

Moreover, the width of the periodic oscillations was smallest for linseed oil + PbO 17 mol% and then increased with the initial PbO content. As an example, the lamellar signal of linseed oil + PbO 50 mol% was broader than that of the linseed oil + PbO 17 mol% and its harmonics, expected at q = 0.30, 0.45, and 0.60 $Å^{-1}$, were not visible. The full width at half maximum (*FWHM*, in Å) of the deconvoluted lamellar signal after baseline subtraction is directly related to the correlation length of the lamellar domains ξ (Å) according to the Scherrer equation [34] :

$$\xi = \frac{2\pi \times K}{FWHM} \#(1)$$

with *K* a constant related to the shape of the lamellar domains, fixed at 0.9 for undefined shape [35]. The correlation length allows to estimate the size of the lamellar domains. This simple approach has already been applied to partially crystallized triglyceride systems in a liquid oil matrix [36,37]. According to the Scherrer equation, the correlation length of the lamellar domains of linseed oil + PbO 17 mol% is of the order of 400 Å (Table 2). That of the most saponified sample, linseed oil + 50 mol%, would be twice as thin, about 200 Å. These estimated values indicate a trend but should be considered with caution, as other factors may come into play and impact the shape of the lamellar signal. Caillé [38] showed that the intensity scattered by a lamellar phase decreases around the positions relative to the maximum of the lamellar signals following a simple power law, related to the thermal undulations of the lamellae along the axis normal to their stacking [39]. These undulations destroy long-range order and arise from the flexibility of the lamellae; in other words, the shape of the lamellar signals provides information about the flexibility of the lamellar organization [40]. Several theoretical papers have improved the Caillé theory, initially valid for an ideal, infinite-dimensional and perfectly oriented lamellar system, by including finite-size and mosaicity. For an isotropic sample consisting of lamellar domains oriented in multiple directions, the structure factor *S(q)* related to the lamellar organization is:

$$S(q) \sim q^{-1+\eta} \#(2)$$

with η a constant called the Caillé parameter (dimensionless) [41]. Qualitatively, the higher η is, the less ordered the system is and the greater its flexibility (low rigidity) [39]. In practice, precisely determining η is a very difficult task, as high resolution is required around the Bragg peaks. Moreover, in the case of saponified oils, the presence of the liquid order signal (noted B) partially overlapped the first order

signal. However, a rough estimate of η can be obtained directly from the number of detected reflections (noted n) [42]:

$$\eta < \frac{1}{n^2} \#(3)$$

The SAXS profile of linseed oil + PbO 17 mol% showed 4 periodic reflections related to the lamellar organization, while for linseed oil + PbO 50 mol%, only the first order signal was clearly visible. According to equation (3), the Caillé parameter increased with the saponification rate, suggesting that the flexibility of the lamellae was greater for the most saponified samples.

In summary, SAXS analyses showed that the supramolecular structuring of lead soaps depended on the saponification rate of the system: the more lead soaps there were in the system, the more compact the lamellar phase, and the thinner and more flexible the lamellar domains. On the other hand, the correlation distance between the unorganized species remained constant (at *ca.* 30 Å) whatever the initial proportion of PbO.

Microscopy

FF-TEM (Freeze-Fracture Transmission Electron Microscopy)

Microscopy observations were then performed on linseed oil + PbO 17 and 50 mol% (Figure 3, S5 and S6), displaying different rheological behaviors and SAXS profiles. As a comparison, images obtained on pure linseed oil are shown Figure S4. FF-TEM on the linseed oil + PbO 17 mol% sample revealed the presence of isolated objects (Figure 3.a, in green) with an average diameter ranging from 1 to 4 µm. These objects were discontinuously dispersed in a continuous unorganized phase. Within the objects, lamellar sheets oriented in different directions were revealed by the fracture (Figure 3.c, in red). In linseed oil + PbO 50 %mol, lamellar domains, of ca. 1 µm-length, were also visible but appeared homogeneously distributed in a continuous phase (Figure 3.b and d., in yellow). Comparable lamellar patterns have already been observed by FF-TEM for example on predominantly monounsaturated aliphatic chain systems [37,43], cellular lipid deposits[44], and surfactants in solution [45,46].

Linseed oil + PbO 17 mol%

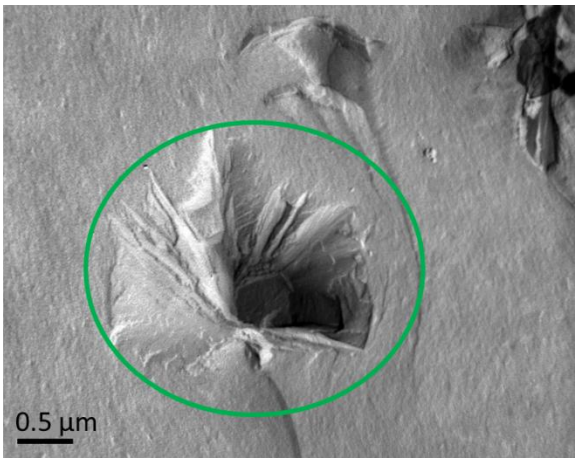

(a)

Linseed oil + PbO 50 mol%

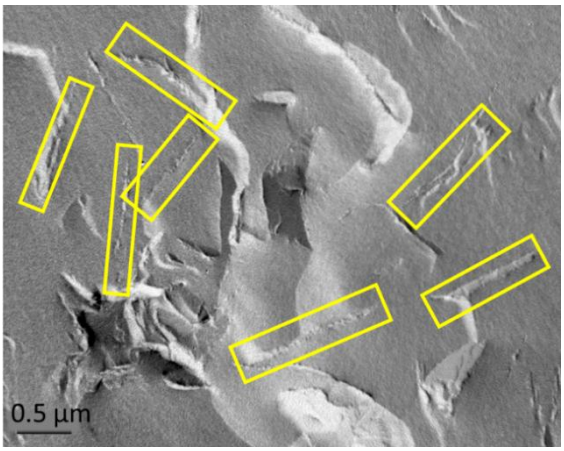

(b)

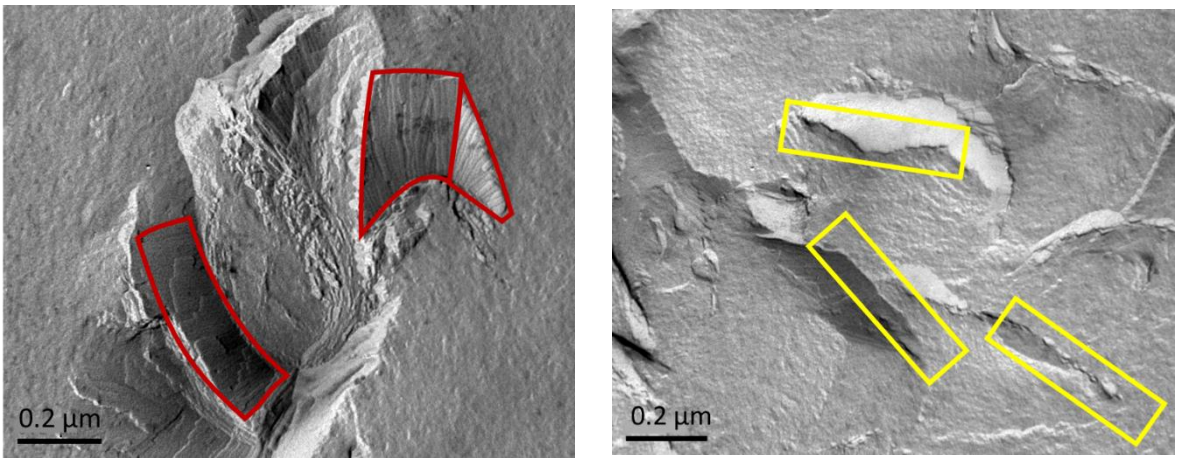

(c) (d)

Figure 3 : FF-TEM images of linseed oil + PbO 17 mol% (a and c) and 50 mol% (b and d). For linseed oil + PbO 17 mol%, several aggregates of lamellar domains are framed in green and some lamellar domains are circled in red. For linseed oil + PbO 50 mol%, some thin lamellar domains are circled in yellow.

DIC (Differential Interference Contrast) microscopy

The images obtained by differential interference contrast microscopy for the two samples also differed, confirming the previous observations: in the linseed oil + PbO 17 mol%, objects with dimensions ranging from 1 to 10 µm were observed, discontinuously dispersed in the unorganized oil phase (Figure 3.c, in green). They probably correspond to the aggregates of lamellar domains identified in FF-TEM. Linseed oil + PbO 50 mol% (Figure 3.d), appeared to be fully textured: the sample was continuously structured, there was no boundary between the continuous unorganized phase and the lamellar domains.

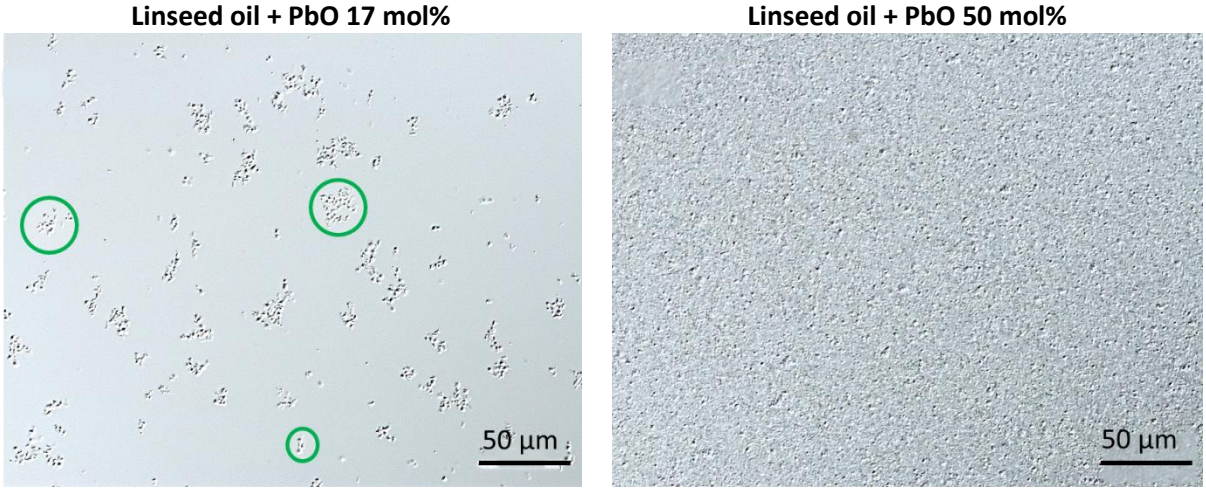

(a) (b)

Figure 4 : DIC microscopy images of linseed oil + PbO (a) 17 mol% and (b) 50 mol%. For the sake of clarity, the contrast and brightness of both images have been identically enhanced.

Discussion

Saponified oils are composed of a wide variety of molecules: tri-, di- and monoglycerides, glycerol, free fatty acids and lead soaps. A minor fraction of all these compounds may also be oxidized, isomerized, or partially crosslinked. In this study, we focused on the architecture of lead soaps at the mesoscopic and supramolecular scale as revealed by SAXS measurements. We have highlighted two

distinct contributions of lead soaps, one characteristic of an unorganized continuous matrix, the other characteristic of a self-assembly of soaps in lamellar domains already described in the literature for model systems only. The lamellar organization of lead soaps has already been demonstrated for pure systems of saturated and monounsaturated soaps [20,23,24,43] : the long-spacing values measured by X-ray diffraction are 45 Å for lead palmitate (C16:0) and 50 to 51 Å for lead stearate (C18:0). These values are of the same order of magnitude as those measured here for saponified oils. It is therefore reasonable to assume that saturated soaps and monounsaturated soaps, whose self-assembly is favored, are the main components of the observed lamellar organization. On the other hand, poly-unsaturated chains have several kinks which hinder their structuring into lamellae [44–46]. For instance, no organization has been demonstrated at room temperature for lead linoleate (C18:2) and linolenate (C18:3). The latter are therefore more likely to remain unorganized within the oil matrix, and the contribution of unorganized species observed in SAXS (Figure 2.a) may originate from polyunsaturated soaps. However, the composition of formulated saponified oils is complex and this schematic representation of the distribution of saturated and unsaturated soaps between the A and B contributions needs to be qualified as several types of aliphatic chains coexist within the same system, in different forms (tri-, di- and monoglycerides, free fatty acids, lead soaps). A lead soap itself is composed of two carboxylates, and can be completely saturated, unsaturated, or mixed (containing saturated and un-saturated chains). The behavior of mixed soaps (e.g. composed of a C18:0 chain and a C18:3 chain) is not clearly established, and we can assume that their ability to take part in a lamellar organization is intermediate to that of saturated soaps (e.g. two C18:0 chains) and unsaturated soaps (e.g. two C18:3 chains).

The initial PbO concentration defines the total proportion of soaps formed and the multi-scale structuring of the resulting saponified oils. We summarize below and in Figure 5 the main results obtained focusing on the two concentrations investigated thanks to SAXS combined to microscopy which exhibit quite a different structuring. We can assume that these differences are linked to a difference in the mobility of the species, due to their different saponification rate:

- The saponification rate of linseed oil + PbO 17% mol is relatively low (see Supporting Information Figure S3, τ_S = 7 % after 10 min heating, 18 % after 120 min). At the start of heating, high species mobility may encourage the self-organization of soaps capable of structuring themselves: the lamellar contribution (A) predominates; the lamellar domains consist of a large number of lamellae and aggregate to form zones distinctly separated from the continuous unorganized phase. The spatial segregation of soaps capable or not to self-assemble is therefore pronounced. Lamellar aggregates remain disconnected in an unorganized matrix, and the viscous behavior predominates as there is no large-scale organization.

- Linseed oil + PbO 50 mol% has a different mesoscopic organization, consisting of thinner lamellar domains and very few aggregates. We can assume that this organization is related to the high concentration of lead soaps in the system (see Supporting Information Figure S3, τ_S = 19 % after 10 min heating, 62 % after 120 min): this high concentration would limit the mobility of soaps. On the one hand, soaps that are able to self-assemble in a lamellar organization, such as saturated soaps, may remain dispersed among the unorganized species. This results in a pronounced unorganized phase (contribution B), and thinner lamellar domains ($\xi \approx 200$ Å). On the other hand, some unsaturated chains in cis

conformation would be embedded in the lamellar organization. This incorporation of unsaturated chains in the lamellar organization would explain why $\overline{d_A}$ is smaller than for linseed oil + PbO 17 mol%, as kinks reduce the end-to-end distance between the terminal carbon atoms of a chain [44]. As an example, the long-spacing of lead oleate (C18:1) is 47 Å [23,24], about 3 Å less than its saturated counterpart. The incorporation of unsaturated chains with double bonds in cis conformation in the lamellar phase would also disrupt the packing of neighboring saturated hydrocarbon and increase the flexibility of the lamellar domain [45,46]. This is consistent with the disappearance of harmonics observed in SAXS for linseed oil + PbO 50 mol% (Figure 2.a), suggesting an increase in the Caillé parameter η [42], and thus a pronounced flexibility of the lamellar organization.

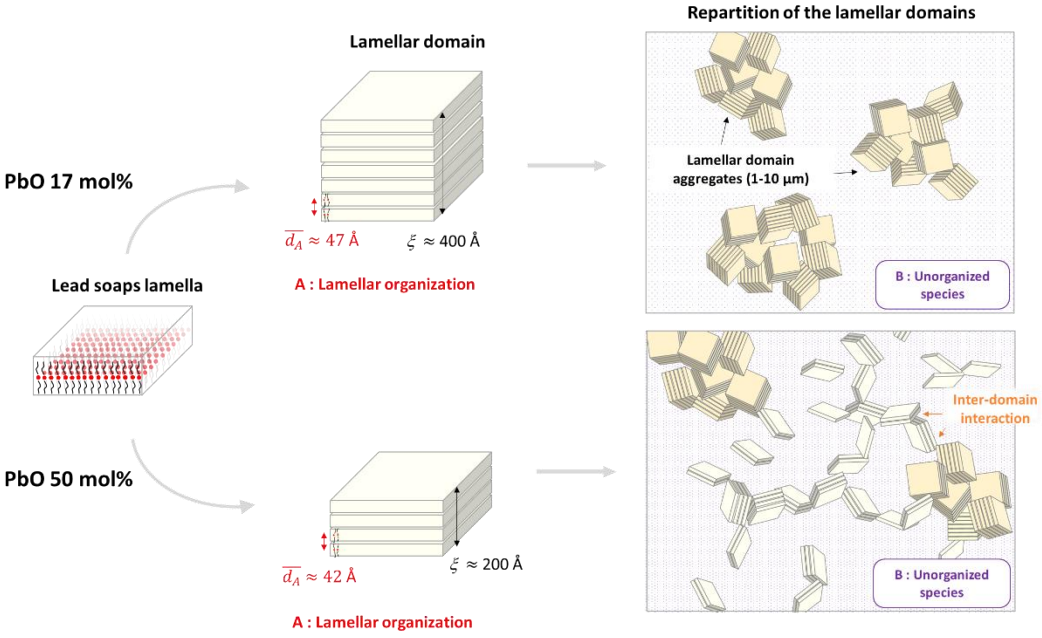

Figure 5 : Simplified schematic representation of the multiscale organization of lead soaps, for linseed oil + PbO 17 %mol% and 50 mol%.

This organization may explain the origin of the viscoelasticity observed specifically for linseed oil + PbO 50 mol%, in which a majority of the lamellar domains are homogeneously distributed in the continuous, unorganized phase. This homogeneous repartition favor the interaction between the lamellar domains on a larger scale: the physical connections between lamellar domains may create a three-dimensional network within the material, as it has been shown for semisolid fat products [47,48]. These systems contain triglycerides that crystallize into lamellar domains and then assemble into larger microstructures until they form a continuous three-dimensional network [36,37]. The schematic architecture that we propose is in agreement with the viscoelastic properties showed on Figure 1 : when linseed oil + PbO 50 mol% is submitted to an oscillatory sweep at low strain, the connections between lamellar domains would be sufficiently numerous for the latter to constrain each other, the network carries the stress and contribute to the elastic properties of the system. Thus, generating viscoelasticity at the macroscopic scale. As evidenced by the oscillatory strain sweep test (Figure 1.b), this network is fragile and breaks beyond a certain strain of about 2 %. If the initial PbO concentration is above 50 mol% (*e.g.* 57 mol%), the formation of lamellar domains is limited and the behavior of the disorganized continuous phase prevail, no viscoelasticity is therefore observed.

Conclusion

For the first time, we show that the macroscopic properties of complex saponified oils are correlated to the organization of lead soaps depending on their concentration. The complementarity of SAXS and microscopy observations revealed the multiscale organization of saponified oils and could explain the differences in rheological behavior observed at the macroscopic scale, as a function of initial PbO concentration. To our knowledge, this is the first report on the structuring of saponified oils representative of "real", complex systems, with previous studies mainly focusing on pure and saturated lead soap systems [43,49–51]. Some of the soaps can be structured to form stacked lamellae, resulting in lamellar domains. It is important to note that these lamellar domains do not consist of rigid and fixed plates, but rather of flexible lamellae that can be subjected to out-of-plane thermal fluctuations. The soaps that are more likely to initiate the structuration are saturated and monounsaturated soaps. Due to reduced soaps mobility, the higher the initial PbO concentration, the smaller the correlation length of the lamellar domains ξ, and the smaller the correlation distance $\overline{d_A}$ between the soap lamellae. The other fraction of soaps remains unorganized and is part of the continuous phase. The distribution of the lamellar domains within this continuous phase (also called oily matrix) also depends on the initial PbO concentration: the lamellar domains of linseed oil + PbO 17 mol% gathered in aggregates of several microns, while those of linseed oil + PbO 50 mol% are mostly homogeneously distributed in the continuous phase, which confers to the sample its viscoelastic properties. Thus, the supramolecular and mesoscopic organization of the saponified oils depends greatly on the initial lead (II) oxide concentration. This organization then drives the macroscopic properties of the oils.

Further research will be carried out to monitor the evolution of these systems along drying, applied as paint films, to describe how, and if, the observed self-organization of lead soaps influence the formation and topology of the paint ionomeric network [52]. This would also shed new light on the aggregation mechanism of saturated lead soaps (the so-called protrusions) which are among the most common alterations observed in oil paintings, providing a better understanding of the environmental conditions and paint formulations that favour them.

Conflicts of interest

There are no conflicts of interest to declare.

Acknowledgments

This project was funded by Sorbonne Université and by the Region Ile de France, DIM-MAP (project RheoPaint). The SAXS experiment was performed with the approval of the SOLEIL Peer Review Committees (BAG No. 20201118). Thomas Bizien is thanked for allowing us to collect data at the workstation, and for his support and assistance during and after the beamtime. We acknowledge Claire Hotton and Laurent Michot from PHENIX (Physicochimie des Electrolytes et Nanosystèmes Interfaciaux, CNRS UMR 8234, Sorbonne Université, 75505 Paris, France) for their fruitful support in sample preparation and SAXS data collection. We warmly thank Nadine Nassif from the LCMCP (Laboratoire de chimie de la matière condensée de Paris, CNRS UMR 7574, Collège de France, Sorbonne Université, 75505 Paris, France) for her precious help concerning our first observations of saponified oils by optical microscopy. This work was supported by the Agence Nationale de la Recherche (Grant ANR-16-CE29-0002-01 CAP-SFC-MS) for GC-MS analysis. We thank Amandine Hueber and Houssein Louati for preliminary results on Fatty Acid Methyl Esters (FAME) analysis by GC-MS.

References

1 M. Faidutti and C. Versini, Le Manuscript de Turquet de Mayerne présenté par M. Faidutti et C. Versini, Pictoria Sculptoria et quae subalternarum artium -1620, Audin Imprimeurs, Lyon, 1967.
2 M. Cotte, E. Checroun, J. Susini, P. Dumas, P. Tchoreloff, M. Besnard and P. Walter, Talanta, 2006, **70**, 1136–1142.
3 C. R. Wold, H. Ni and M. D. Soucek, Chem. Mater., 2001, **13**, 3032–3037.
4 L. de Viguerie, PhD thesis, Université Pierre et Marie Curie, 2009.
5 L. Laporte, G. Ducouret, F. Gobeaux, A. Lesaine, C. Hotton, T. Bizien, L. Michot and L. de Viguerie, J. Colloid Interface Sci., 2023, **633**, 566–574.
6 L. de Viguerie, G. Ducouret, M. Cotte, F. Lequeux and P. Walter, Colloids Surf., 2008, **331**, 119–125.
7 J. Salvant Plisson, L. de Viguerie, L. Tahroucht, M. Menu and G. Ducouret, Colloids Surf., 2014, **458**, 134–141.
8 J. Bieleman and R. Lomölder, in Additives for Coatings, John Wiley & Sons, New York, 2007, pp. 201–256.
9 M. D. Soucek, T. Khattab and J. Wu, Prog. Org. Coat., 2012, **73**, 435–454.
10 L. de Viguerie, P. A. Payard, E. Portero, P. Walter and M. Cotte, Prog. Org. Coat., 2016, **93**, 46–60.
11 L. Dubrulle, R. Lebeuf, L. Thomas, M. Fressancourt-Collinet and V. Nardello-Rataj, Prog. Org. Coat., 2017, **104**, 141–151.
12 R. M. A. Heeren, J. J. Boon, P. Noble and J. Wadum, in ICOM-CC Triennial meeting (12th), Lyon, 29 August-3 September 1999: preprints., James & James, London, 1999, vol. 1, pp. 228–233.
13 C. Higgitt, M. Spring and D. Saunders, The National Gallery Technical Bulletin, 2003, **24**, 75–95.
14 M. J. Plater, B. M. de Silva, T. Glebrich, M. B. Hursthouse, C. L. Higgitt and D. R. Saunders, Polyhedron, 2003, **22**, 3171–3179.
15 P. Noble, in Metal Soaps in Art : Conservation and Research, Springer International Publishing, Cham, 2019, pp. 1–22.
16 E. Platania, N. L. W. Streeton, A. Vila, D. Buti, F. Caruso and E. Uggerud, Spectrochimica Acta Part A: Molecular and Biomolecular Spectroscopy, 2020, **228**, 117844.
17 F. C. Izzo, M. Kratter, A. Nevin and E. Zendri, ChemistryOpen, 2021, **10**, 904–921.
18 R. W. Corkery, Langmuir, 1997, **13**, 3591–3594.
19 K. Binnemans, R. Van Deun, B. Thijs, I. Vanwelkenhuysen and I. Geuens, Chem. Mater., 2004, **16**, 2021–2027.
20 F. J. Martínez-Casado, M. Ramos-Riesco, J. A. Rodríguez-Cheda, M. I. Redondo-Yélamos, L. Garrido, A. Fernández-Martínez, J. García-Barriocanal, I. da Silva, M. Durán-Olivencia and A. Poulain, Phys. Chem. Chem. Phys., 2017, **19**, 17009–17018.
21 E. Kočí, J. Rohlíček, L. Kobera, J. Plocek, S. Švarcová and P. Bezdička, Dalton Trans., 2019, **48**, 12531–12540.
22 F. Martínez-Casado, J. A. Rodríguez-Cheda, M. Ramos-Riesco, M. Redondo-Yélamos, F. Cucinotta and A. Fernández-Martínez, in Metal Soaps in Art: Conservation and Research, Springer, Cham, 2019, pp. 227–239.
23 M.-C. Corbeil and L. Robinet, Powder Diffr., 2002, **17**, 52–60.
24 L. Robinet and M.-C. Corbeil, Stud Conserv., 2003, **48**, 23–40.
25 J. D. J. van den Berg, PhD thesis, University of Amsterdam, 2002.
26 T. Mungure and E. Birch, SOP Transactions on Analytical Chemistry, 2014, **2**, 48–61.
27 I. Bonaduce, L. A. Carlyle, M. P. Colombini, C. Duce, C. Ferrari, E. Ribechini, P. Selleri and M. R. Tiné, J. Therm. Anal. Calorim., 2012, **107**, 1055–1066.
28 J. C. Martin, M. Nour, F. Lavillonnière and J. L. Sébédio, JAOCS, 1998, **75**, 1073–1078.
29 A. A. Christy, Lipids, 2009, **44**, 1105–1112.
30 J. D. J. van den Berg, N. D. Vermist, L. A. Carlyle, M. Holcapek and J. B. Boon, J. Sep. Sci., 2004, **27**, 181–199.

31 J. C. Martin, M. C. Dobarganes, M. Nour, G. Marquez-Ruiz, W. W. Christie, F. Lavillonnière and J. L. Sébédio, JAOCS, 1998, **75**, 1065–1071.
32 M. Cotte, E. Checroun, W. De Nolf, Y. Taniguchi, L. de Viguerie, M. Burghammer, P. Walter, C. Rivard, M. Salomé, K. Janssens and J. Susini, Stud. Conserv., 2017, **62**, 2–23.
33 Y. Li, A. S. Fabiano-Tixier, K. Ruiz, A. Rossignol Castera, P. Bauduin, O. Diat and F. Chemat, Food Chem., 2015, **173**, 873–880.
34 H. P. Klug and L. E. Alexander, X-Ray Diffraction Procedures: For Polycrystalline and Amorphous Materials, John Wiley & Sons, New York, 2nd edn., 1974.
35 N. C. Acevedo and A. G. Marangoni, Cryst. Growth Des., 2010, **10**, 3327–3333.
36 N. C. Acevedo and A. G. Marangoni, Annu. Rev. Food Sci. Technol., 2015, **6**, 71–96.
37 P. R. Ramel, E. D. Co, N. C. Acevedo and A. G. Marangoni, Prog. Lipid Res., 2016, **64**, 231–242.
38 A. Caillé, C. R. Acad. Sci., 1972, **274**, 891–893.
39 F. Castro-Roman, L. Porcar, G. Porte and C. Ligoure, Eur. Phys. J. E, 2005, **18**, 259–272.
40 I. W. Hamley, Soft Matter, 2022, **18**, 711–721.
41 V. M. Kaganer, B. I. Ostrovskii and W. H. de Jeu, Phys. Rev. A, 1991, **44**, 8158–8166.
42 C. R. Safinya, D. Roux, G. S. Smith, S. K. Sinha, P. Dimon, N. A. Clark and A. M. Bellocq, Phys. Rev. Lett., 1986, **57**, 2718–2721.
43 M. W. Rigler, I. L. Roth, D. Kritchevsky and J. S. Patton, J Am Oil Chem Soc, 1983, **60**, 1291–1298.
44 H. W. Meyer and W. Richter, Micron, 2001, **32**, 615–644.
45 P. Versluis, J. C. van de Pas and J. Mellema, Langmuir, 1997, **13**, 5732–5738.
46 Y. Zhao, Y. Yan, L. Jiang, J. Huang and H. Hoffmann, Soft Matter, 2009, **5**, 4250–4255.
47 J. J. Hermans, K. Keune, A. van Loon, M. J. N. Stols-Witlox, R. W. Corkery and P. D. Iedema, in Building strong culture through conservation, J. Bridgland, Melbourne, 2014, pp. 1603–1612.
48 A. L. Rabinovich and P. O. Ripatti, Biochim. Biophys. Acta, Lipids Lipid Metab., 1991, **1085**, 53–62.
49 K. Gawrisch, N. V. Eldho and L. L. Holte, Lipids, 2003, **38**, 445–452.
50 J. M. S. Law, D. H. Setiadi, G. A. Chass, I. G. Csizmadia and B. Viskolcz, J. Phys. Chem. A, 2005, **109**, 520–533.
51 S. S. Narine and A. G. Marangoni, Phys. Rev. E, 1999, **59**, 1908–1920.
52 D. Tang and A. G. Marangoni, Trends Food Sci. Technol., 2007, **18**, 474–483.
53 F. Martínez Casado, M. Riesco and J. Cheda, J. Therm. Anal. Calorim., 2012, **108**, 399.
54 J. Catalano, V. D. Tullio, M. Wagner, N. Zumbulyadis, S. A. Centeno and C. Dybowski, Magn. Reson. Chem., 2020, **58**, 798–811.
55 J. Hermans, L. Zuidgeest, P. Iedema, S. Woutersen and K. Keune, Phys. Chem. Chem. Phys., 2021, **23**, 22589–22600.
56 J. Hermans, K. Keune, A. van Loon, R. W. Corkery and P. D. Iedema, RSC Adv., 2016, **6**, 93363–93369.
57 J. La Nasa, F. Modugno, M. Aloisi, A. Lluveras-Tenorio and I. Bonaduce, Anal. Chim. Acta, 2018, **1001**, 51–58.
58 J. La Nasa, A. Lluveras-Tenorio, F. Modugno and I. Bonaduce, Heritage Sci., 2018, **6**, 57.

Supporting Information

Table S1: Final saponification rate τ_S of linseed oil samples heated at 150°C with PbO as a function of the initial amount of PbO.

PbO (mol%)	4	17	31	50	57
τ_S (%)	3 ± 0	18 ±2	33 ± 3	59 ± 4	72 ± 1

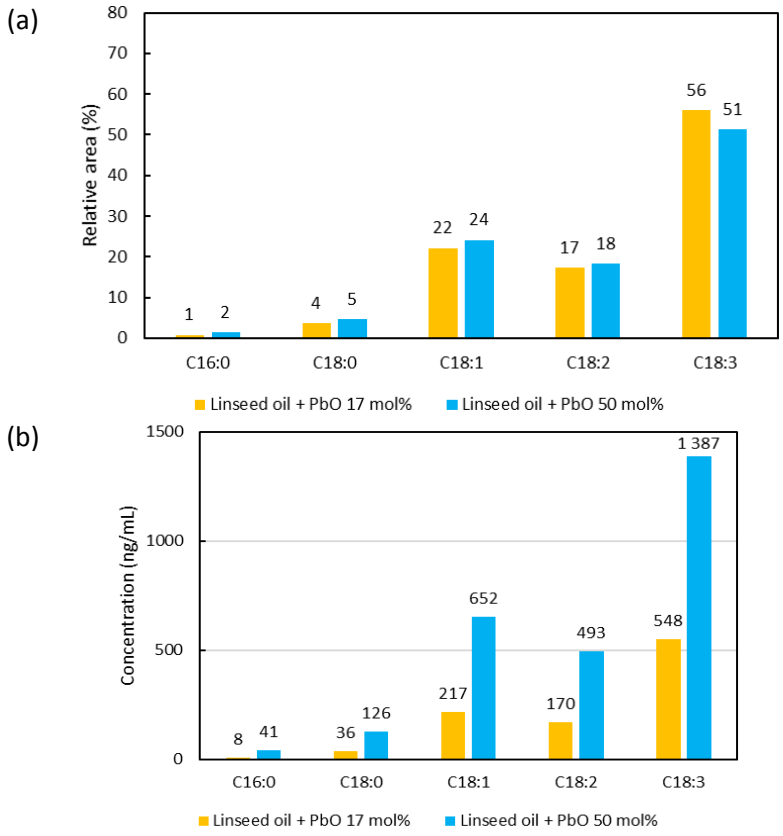

Figure S1: (a) Distribution of fatty acid chains from lead soaps and free fatty acids obtained by GC-MS (Gas Chromatography – Mass Spectrometry) after derivatization with BSTFA. The method used is described below. (b) corresponding absolute concentration in ng/ml.

Samples of saponified oils were weighed into a flask and successive dilutions in heptane were performed to obtain a 40 µg/L concentrated solution. 20 µL of a BSTFA (bis(trimethylsilyl)trifluoroacetamide) solution (Supelco) were added to 150 µL of the diluted solution, and the mixture was heated at 90°C (± 5°C) for 80 min. The use of BSTFA as a derivatizing agent allows to probe specifically the distribution of the fatty acid chains from soaps and free fatty acids [53,54]. The resulting solution was delivered to the injector of an Agilent 7890B-GC system (Agilent Technologies) coupled to an Agilent MSD 5977B single quadrupole mass spectrometer (Agilent Technologies). Volatile compounds were separated with a HP-5MS column (30 m x 0.25 mm x 0.25 µm, Agilent Technologies) subjected to the following temperature gradient: 80°C for 2 min, then 15°C/min to 280°C, followed by an isotherm at 280°C for 10 min. For all samples, the injection was performed in splitless mode. The injection volume was 1 µL, the injector temperature was set at 280°C and the flow rate of the carrier gas (helium) at 1.5 mL/min. For detection, electron impact ionization was performed. The electron energy was 70 eV. The temperature of the ion source was

250°C, that of the quadrupole 150°C. The range of m/z ratios scanned was 50 to 700, at a frequency of 2.3 scans/s. Absolute quantification of free fatty acids have been performed using calibration curves from 2 to 1000 ng/mL after sample derivatization.

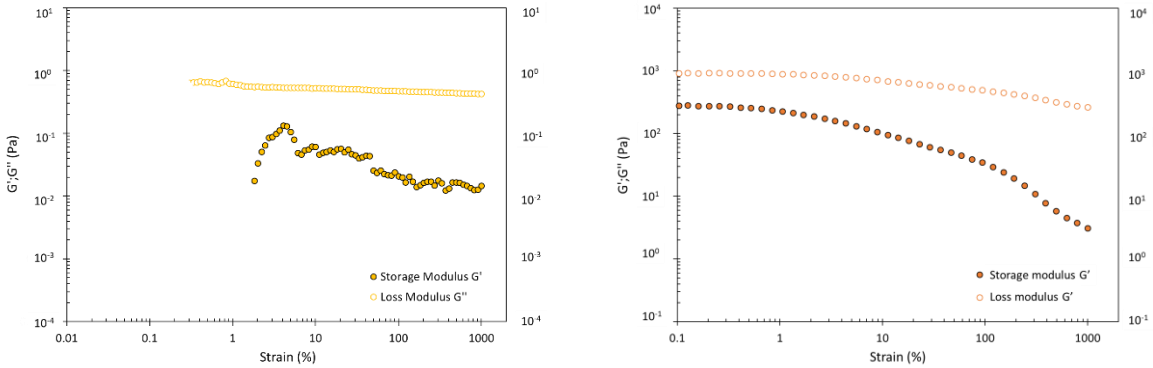

Figure S2: Oscillatory strain sweep test from 0.05 to 1000 % (f = 1 Hz) on linseed oil + PbO (a) 17 and (b) 57 mol%.

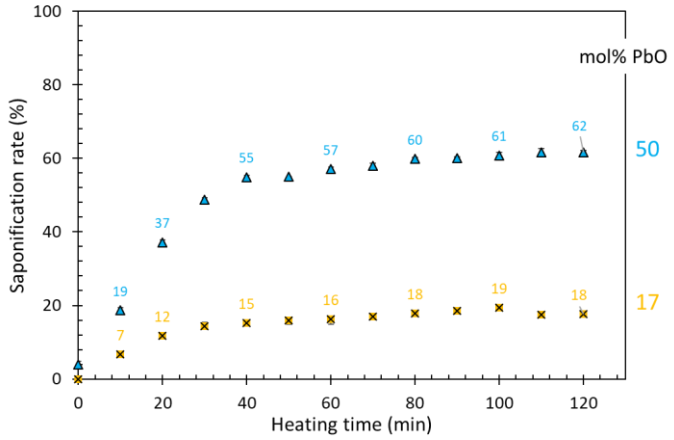

Figure S3: Evolution of saponification rate during heating of linseed oil containing 17 and 50 mol% PbO. Error bars are included in the size of the symbols used.

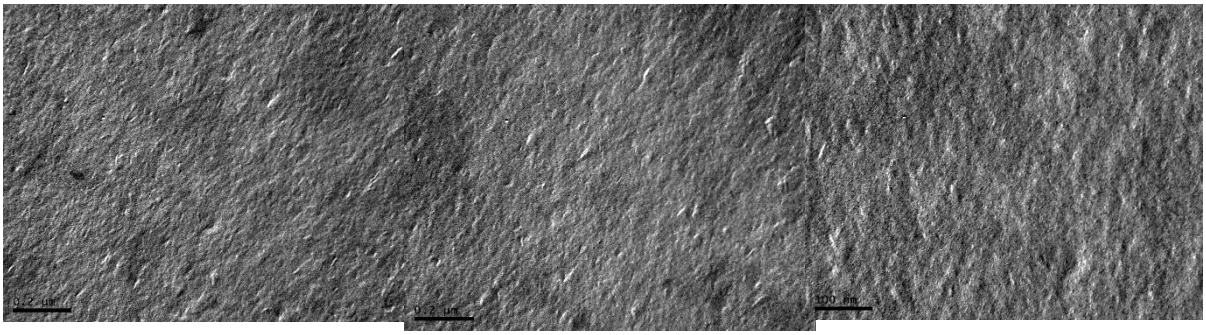

Figure S4: FF-TEM images of linseed oil alone.

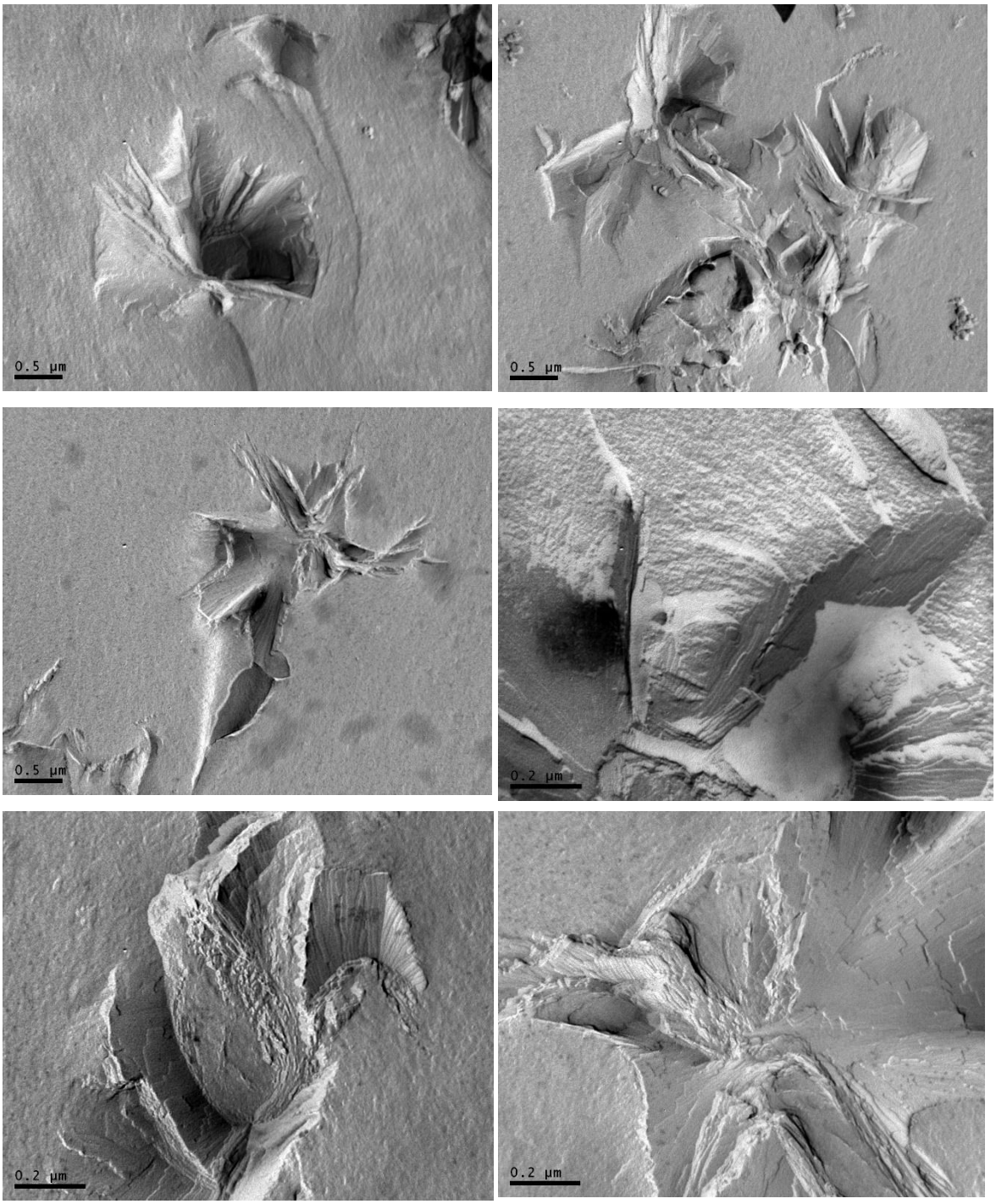

Figure S5: FF-TEM images of linseed oil + PbO 17 mol%

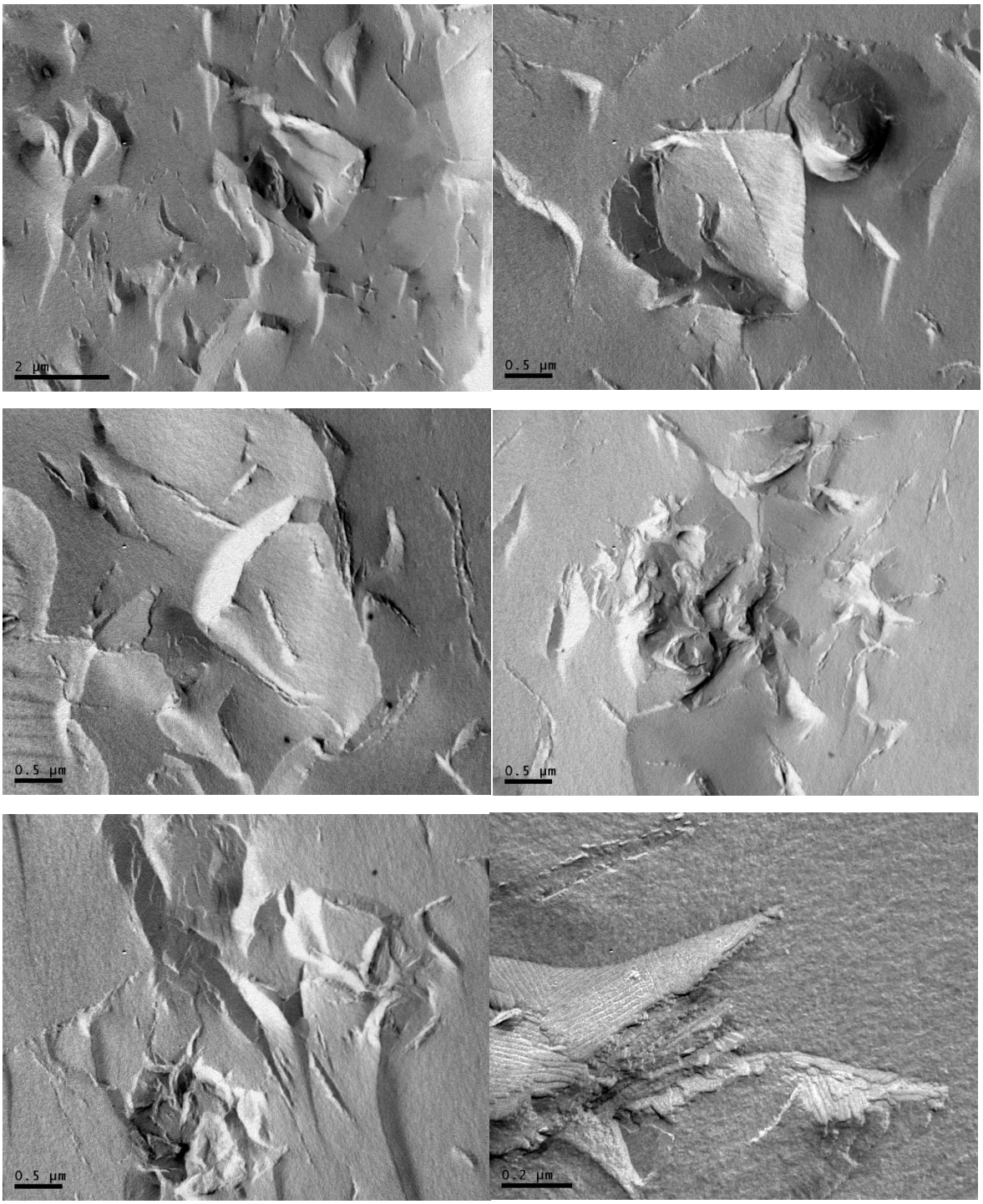

Figure S6: FF-TEM images of linseed oil + PbO 50 mol%